# Contribution of the $4f$-core-excited states in determination of atomic properties in the promethium isoelectronic sequence

U. I. Safronova and A. S. Safronova
*Physics Department, University of Nevada, Reno, Nevada 89557, USA*

P. Beiersdorfer
*Physics Division, Lawrence Livermore National Laboratory, Livermore, California 94550, USA*

(Received 12 May 2013; published 18 September 2013)

The atomic properties of Pm-like ions were comprehensively studied using relativistic atomic codes. Excitation energies of the $4f^{14}nl$ (with $nl = 5s$, $6s$, $5p$, $6p$, $5d$, $6d$, and $5f$) states in Pm-like ions with nuclear charge $Z$ ranging from 74 to 100 are evaluated within the framework of relativistic many-body theory (RMBPT). First- and second-order Coulomb energies and first- and second-order Breit corrections to the energies are calculated. Two alternative treatments of the Breit interaction are investigated. In the first approach we omit Breit contributions to the Dirac-Fock potential and evaluate Coulomb and Breit-Coulomb corrections through second order perturbatively. In the second approach were included both Coulomb and Breit contributions on the same footing via the Breit-Dirac-Fock potential and then treat the residual Breit and Coulomb interactions perturbatively. The results obtained from the two approaches are compared and discussed. The important question of what is the ground state in Pm-like ions was answered. Properties of the $4f$-core-excited states are evaluated using the multiconfiguration relativistic Hebrew University Lawrence Livermore atomic code (HULLAC code) and the Hartree-Fock-relativistic method (COWAN code). We evaluate excitation energies and transition rates in Pm-like ions with nuclear charge $Z$ ranging from 74 to 92. Our large scale calculations include the following set of configurations: $4f^{14}5s$, $4f^{14}5p$, $4f^{13}5s^2$, $4f^{13}5p^2$, $4f^{13}5s5p$, $4f^{12}5s^25p$, $4f^{12}5s5p^2$, and $4f^{12}5p^3$. Trends of excitation energies as function of $Z$ are shown graphically for selected states. Excitation energies, transition rates, and lifetimes in Pm-like tungsten are evaluated with additional inclusion of the $4f^{11}5s^25p^2$, $4f^{11}5s5p^3$, $4f^{10}5s^25p^3$, and $4f^{10}5s5p^4$ configurations. This represents an unusual example of an atomic system where the even-parity complex $[4f^{14}5s + 4f^{13}5s5p + 4f^{12}5s5p^2 + 4f^{11}5s5p^3 + 4f^{10}5s5p^4]$ and the odd-parity complex $[4f^{14}5p + 4f^{13}5s^2 + 4f^{12}5s^25p + 4f^{11}5s^25p^2 + 4f^{10}5s^25p^3]$ include so different configurations. Wavelengths of the $4f^{14}5s\ ^2S_{1/2}$-$4f^{14}5p\ ^2P_J$ transition obtained by the COWAN, HULLAC, and RMBPT codes are compared with other theoretical results and available measurements.

DOI: 10.1103/PhysRevA.88.032512 PACS number(s): 31.15.ag, 31.15.am, 31.15.vj, 31.15.aj

## I. INTRODUCTION

Achieving an accurate description of complex correlations in atomic and molecular structure is of fundamental importance and one of the goals of current atomic physics research. Ions with an open $4f$ shell are prime examples of highly correlated systems, and an accurate representation of their structure is a largely unsolved problem. In fact, even the important question "at what ionic state is $4f^{14}5s$ the ground state of Pm-like ions, i.e., of ions with 61 remaining electrons?" has long remained unanswered. However, correct knowledge of atomic systems with an open $4f$ shell is of high importance, as recently demonstrated in the development of a frequency standard based on the $4f^{13}6s^2$ configuration in ytterbium with 69 remaining electrons [1], or in the development of a sensitive indicator for measuring the variation of $\alpha$ based on similar configurations, but with $5s$ valence electrons in Pm-like or Nd-like iridium [2].

The first theoretical prediction of the $4f^{14}5s\ ^2S_{1/2}$-$4f^{14}5p\ ^2P_{1/2}$ and $4f^{14}5s\ ^2S_{1/2}$-$4f^{14}5p\ ^2P_{3/2}$ wavelengths and the $4f^{14}5p\ ^2P_{1/2}$ and $4f^{14}5p\ ^2P_{3/2}$ lifetimes in Pm-like ions was presented by Curtis and Ellis [3]. The Hartree-Fock (HF) calculations showed that in Pm-like $W^{13+}$, $Ir^{16+}$, $Au^{18+}$, $Pb^{21+}$, and $U^{31+}$ the dominant resonance lines were the $5s$-$5p$ doublets in the range $\lambda = 100$–$400$ Å. Theodosiou and Raftopoulos [4] performed a fully relativistic calculation, using the Dirac-Fock approximation (DF) to evaluate energies of the $4f^{14}nl_j$ ($nl_j = 5s_{1/2}$, $5p_{1/2}$, $5p_{3/2}$, $5d_{3/2}$, $5d_{5/2}$, $4f_{5/2}$, and $4f_{7/2}$) levels for Pm-like $W^{13+}$, $Ir^{16+}$, $Au^{18+}$, $Pb^{21+}$, and $U^{31+}$ ions. A small difference was found for the wavelengths of the $5s$-$5p$ transitions and the $4f^{14}5p\ ^2P_{3/2}$ lifetimes between their DF results [4] and the HF results [3]. Theodosiou and Raftopoulos [4] answered the question, discussed in Ref. [3], at what ionic state $4f^{14}5s$ is the ground state of Pm-like ions by predicting that this will happen first for $Ir^{16+}$.

Twenty five years later, the large set of the $4f$-core-excited states ($4f^{13}5s^2$, $4f^{13}5p^2$, $4f^{13}5s5p$, $4f^{12}5s^25p$, $4f^{12}5s5p^2$, $4f^{12}5p^3$) was used by Vilkas *et al.* [5] to evaluate wavelengths and lifetimes in Pm-like ions. It was found that the $4f^{14}5s\ ^2S_{1/2}$ level is the ground state from $Z = 78$ onwards ($Pt^{17+}$), i.e., one charge higher than it was thought to be in [4]. Numerical values for the excitation energies and lifetimes obtained by the multireference Møller-Plesset (MR-MP) approach were presented [5] in the case of Pm-like $W^{13+}$ ion. Kramida and Shirai [6] confirmed that the $4f^{13}5s^2\ ^2F_{7/2}$ level is the ground state of Pm-like $W^{13+}$ ion. It was also found that the first excited state $4f^{13}5s^2\ ^2F_{5/2}$ was separated from the ground state by approximately 18 000 $cm^{-1}$ [6]. In his review [7], Kramida estimated the accuracy

 ©2013 American Physical Society

of theoretical calculations [5] and experimental measurements [8,9] of the $4f^{14}5s\ ^2S_{1/2}$-$4f^{14}5p\ ^2P_{1/2}$ and $4f^{14}5s\ ^2S_{1/2}$-$4f^{14}5p\ ^2P_{3/2}$ transitions, and he noted the importance of including two additional configurations ($4f^{11}5s^25p^2$ and $4f^{10}5s^25p^3$) in the calculations presented by Vilkas *et al.* [5]. If the configurations $4f^{11}5s^25p^2$ and $4f^{10}5s^25p^3$ were not included in the calculations in [5], it would affect the calculated energies of odd-parity levels that were predicted by Kramida [7].

In the present work we have employed several relativistic atomic codes to study Pm-like ions. We report results of *ab initio* calculation of the excitation energies in Pm-like ions using the relativistic many-body perturbation theory (RMBPT). We consider these ions as systems with a closed $[\mathrm{Kr}]4d^{10}4f^{14}$ core and one electron above the core as $[\mathrm{Kr}]4d^{10}4f^{14}nl$ states. We use a complete set of DF wave functions on a nonlinear grid generated using B splines [10] constrained to a spherical cavity. The basis set consists of 50 splines of order 9 for each value of the relativistic angular quantum number $\kappa$.

Properties of the $4f$-core-excited states are evaluated using the multiconfiguration relativistic Hebrew University Lawrence Livermore atomic code (HULLAC code) and the Hartree-Fock-relativistic method (COWAN code). We evaluate excitation energies and transition rates in Pm-like ions with nuclear charge $Z$ ranging from 74 to 92. Our large scale calculations include the following set of configurations: $4f^{13}5s^2$, $4f^{13}5p^2$, $4f^{13}5s5p$, $4f^{12}5s^25p$, $4f^{12}5s5p^2$, and $4f^{12}5p^3$.

We present excitation energies, transition rates, and lifetimes for the specific case of Pm-like tungsten. This emphasis is derived from the prospect that tungsten will be abundant in the plasmas generated by the ITER (Latin, "the way") tokamak, which is currently under construction in France, as well as in many present-day plasma devices that have started to experiment with "ITER-like" plasma-facing components, which often include tungsten. This renewed experimental interest in tungsten spectroscopy is illustrated by many recent publications [11–25]. For example, an interpretation of the spectral emission in the 20 nm region from tungsten ions was recently presented by Suzuki *et al.* [13,14]. These extreme ultraviolet spectra were produced in the large helical device at the National Institute for Fusion Science. A quasicontinuum spectral feature arising from an unresolved transition array was observed around 20 nm in plasmas with temperatures below 1 keV. Atomic structure calculations for tungsten ions with open $5p$, $5s$, and $4f$ subshells ($W^{7+}$-$W^{27+}$) were needed to interpret the observed feature.

We show that in the case of $W^{13+}$ ion, the energies of the $4f^{11}5s^25p^2$ and $4f^{10}5s^25p^3$ are distributed inside the interval between the $4f^{14}5s\ ^2S_{1/2}$ and $4f^{14}5p\ ^2P_J$ energies. This is an example of a very unusual atomic system, in which the even-parity complex $[4f^{14}5s + 4f^{13}5s5p + 4f^{12}5s5p^2 + 4f^{11}5s5p^3 + 4f^{10}5s5p^4]$ and the odd-parity complex $[4f^{14}5p + 4f^{13}5s^2 + 4f^{12}5s^25p + 4f^{11}5s^25p^2 + 4f^{10}5s^25p^3]$ include grossly different configurations. Such an unusual atomic system was not investigated before. We present synthetic spectra for the $[4f^{14}5s + 4f^{13}5s5p + 4f^{12}5s5p^2] \leftrightarrow [4f^{14}5p + 4f^{13}5s^2 + 4f^{12}5s^25p]$ transitions in both Pm-like $W^{13+}$ and Pm-like $Au^{18+}$.

## II. ENERGIES AND WAVELENGTHS WITH INCLUSION OF THE $4f^{14}nl$ STATES IN Pm-LIKE IONS

The excitation energies of the $4f^{14}nl$ (with $nl = 5s$, $6s$, $5p$, $6p$, $5d$, $6d$, and $5f$) states in Pm-like ions with nuclear charge $Z$ ranging from 74 to 100 are evaluated within the framework of relativistic many-body theory (RMBPT). At first we decided to exploit the single-double all-order (SD) method that was used previously [26,27] for Au-like and Fr-like ions. We found that a convergence problem affected the SD method for calculations of energies in Pm-like $W^{13+}$ ion. This convergence problem is due to an unstable $4f^{14}$ core because of the large contribution of $4f$-core excitations. As a result we decided to limit our study of atomic properties of the excited $4f^{14}nl$ states in Pm-like ions to applying the second-order RMBPT approximation.

The calculations are carried out using a basis set of Dirac-Fock (DF) orbitals. The orbitals used in the present calculations are obtained as linear combinations of B splines. These B-spline basis orbitals are determined using the method described in Ref. [10]. We employ 50 B splines of order 9 for each single-particle angular momentum state, and we include all orbitals with orbital angular momentum $l \leqslant 8$ in our basis set.

In Table I we illustrate the relative size of various contributions for energies of the $4f^{14}nl$ (with $nl = 5s$, $6s$, $5p$, $6p$, $5d$, $6d$, and $5f$) states using the example of Pm-like $W^{13+}$. First- and second-order Coulomb energies and first- and second-order Breit corrections to energies are calculated. Two alternative treatments of the Breit interaction are investigated.

The first-order and second-order Breit corrections $B^{(1)}$ and $B^{(2)}$ given in columns 4 and 5 of Table I are obtained with the Dirac-Fock potential when the Breit contributions are omitted. We evaluate Coulomb and Breit-Coulomb corrections through the second order perturbatively. The alternative treatments include both Coulomb and Breit contributions to the Breit-Dirac-Fock potential and then treatment of the residual Breit and Coulomb interactions perturbatively. In this approximation the first-order Breit corrections $B^{(1)}$ is equal to zero. The value of the second-order Breit corrections $BB^{(2)}$ given in column 10 of Table I is smaller than the value of $B^{(2)}$ (column 5) since the RPA diagram was removed from the $B^{(2)}$ correction (see for details Sect. III of Ref. [28]). A very small difference (less than 0.01%) in the $E^{(2)}$ evaluated in the Dirac-Fock potential or in the Breit-Dirac-Fock potential (compare the $E^{(2)}$ and the $E^{(2B)}$ values given in columns 3 and 8 of Table I) is found. The largest difference between the two approximations is in the Breit correction as well as in the DF and BDF ($E^{(\mathrm{DF})}$ $E^{(\mathrm{BDF})}$) energies.

The wavelengths of the $4f^{14}5s\ ^2S_{1/2}$-$4f^{14}5p\ ^2P_{1/2}$ and $4f^{14}5s\ ^2S_{1/2}$-$4f^{14}5p\ ^2P_{3/2}$ transition in Pm-like ions with $Z = 74$–$100$ are listed in Table II. The wavelengths given in columns "RMBPT" and "RMBPTB" are calculated in the second-order approximation with a Dirac-Fock (DF) and Breit-Dirac-Fock (BDF) potentials, respectively. The difference between two results is about 0.01%–0.03% for the $4f^{14}5s\ ^2S_{1/2}$-$4f^{14}5p\ ^2P_{1/2}$ transition and 0.02%–0.07% for the $4f^{14}5s\ ^2S_{1/2}$-$4f^{14}5p\ ^2P_{3/2}$ transition.

In column "Theory" of Table II we present the results obtained by the multireference Møller-Plesset (MR-MP)

TABLE I. Energies (in $cm^{-1}$) calculated with a Dirac-Fock (DF) or a Breit-Dirac-Fock (BDF) potential for Pm-like $W^{13+}$. Zeroth-order energies $E^{(DF)}$ and $E^{(BDF)}$, second-order Coulomb energies $E^{(2)}$ and $E^{(2B)}$, first-order $B^{(1)}$ and second-order Breit-Coulomb ($B^{(2)}$ and $BB^{(2)}$) corrections, and Lamb shift corrections $E_{LS}$ are listed separately, followed by the total energies ($E^{(2)}_{tot} = E^{(DF)} + E^{(2)} + B^{(1)} + B^{(2)} + E_{LS}$ and $E^{(2B)}_{tot} = E^{(BDF)} + E^{2B} + BB^{(2)} + E_{LS}$). The value of the infinite mass Rydberg constant used to convert numerical data from a.u. to $cm^{-1}$ is Ry = 10 973.7316.

| $nlj$ | $E^{(DF)}$ | $E^{(2)}$ | $B^{(1)}$ | $B^{(2)}$ | $E_{LS}$ | $E^{(2)}_{tot}$ | $E^{(BDF)}$ | $E^{(2B)}$ | $BB^{(2)}$ | $E^{(2B)}_{tot}$ |
|---|---|---|---|---|---|---|---|---|---|---|
| $5s_{1/2}$ | −2 440 665 | −28 939 | 3093 | −2549 | 1052 | −2 468 007 | −2 438 708 | −28 918 | −52 | −2 466 628 |
| $5p_{1/2}$ | −2 172 710 | −27 298 | 3901 | −2269 | −30 | −2 198 406 | −2 169 811 | −27 215 | −57 | −2 197 113 |
| $5p_{3/2}$ | −2 060 939 | −24 527 | 2626 | −1975 | 41 | −2 084 775 | −2 059 194 | −24 463 | −42 | −2 083 658 |
| $5d_{3/2}$ | −1 651 209 | −19 011 | 1593 | −1583 | 0 | −1 670 209 | −1 650 343 | −18 959 | −25 | −1 669 327 |
| $5d_{5/2}$ | −1 632 523 | −18 298 | 1248 | −1566 | 0 | −1 651 138 | −1 632 000 | −18 262 | −31 | −1 650 292 |
| $5f_{5/2}$ | −1 181 195 | −10 726 | 565 | −1108 | 0 | −1 192 464 | −1 181 133 | −10 707 | −11 | −1 191 851 |
| $5f_{7/2}$ | −1 177 521 | −10 567 | 442 | −1123 | 0 | −1 188 768 | −1 177 593 | −10 555 | −15 | −1 188 163 |
| $6s_{1/2}$ | −1 333 312 | −15 056 | 1153 | −876 | 287 | −1 347 805 | −1 332 567 | −14 997 | −24 | −1 347 302 |
| $6p_{1/2}$ | −1 219 385 | −12 365 | 1527 | −826 | −12 | −1 231 060 | −1 218 240 | −12 320 | −27 | −1 230 598 |
| $6p_{3/2}$ | −1 174 510 | −11 038 | 1066 | −760 | 10 | −1 185 231 | −1 173 799 | −11 010 | −21 | −1 184 820 |
| $6d_{3/2}$ | −991 835 | −8 773 | 713 | −683 | 0 | −1 000 578 | −991 447 | −8 714 | −14 | −1 000 175 |
| $6d_{5/2}$ | −983 417 | −8 291 | 559 | −682 | 0 | −991 831 | −983 185 | −7 843 | −17 | −991 045 |

TABLE II. Wavelengths (in Å) of the $4f^{14}5s\ ^2S_{1/2}$-$4f^{14}5p\ ^2P_{1/2}$ and $4f^{14}5s\ ^2S_{1/2}$-$4f^{14}5p\ ^2P_{3/2}$ transitions in Pm-like ions. The wavelengths given in columns "RMBPT" and "RMBPTB" are calculated in the second-order approximation with a Dirac-Fock (DF) and Breit-Dirac-Fock (BDF) potentials, respectively. The Hartree-Fock relativistic method implemented in the COWAN code was used to evaluate the wavelengths listed in column COWAN. Our results are compared with theoretical results obtained by the MR-MP approach (column "Theory") and experimental (column "Expt.") values presented by Vilkas *et al.* [5].

| $Z$ | RMBPT | RMBPTB | COWAN | Theory | Expt. | RMBPT | RMBPTB | COWAN | Theory | Expt. |
|---|---|---|---|---|---|---|---|---|---|---|
| | $4f^{14}5s\ ^2S_{1/2}$-$4f^{14}5p\ ^2P_{1/2}$ transition | | | | | $4f^{14}5s\ ^2S_{1/2}$-$4f^{14}5p\ ^2P_{3/2}$ transition | | | | |
| 74 | 370.92 | 371.04 | 367.95 | 369.45 | 365.3 | 260.94 | 261.12 | 260.83 | 261.06 | 258.2 |
| 75 | 351.56 | 351.65 | 349.56 | 350.22 | | 242.73 | 242.88 | 242.80 | 237.82 | |
| 76 | 334.24 | 334.32 | 331.78 | 333.26 | | 226.38 | 226.52 | 225.21 | 221.42 | |
| 77 | 318.50 | 318.56 | 323.20 | 320.78 | | 211.55 | 211.66 | 212.82 | 212.94 | |
| 78 | 304.08 | 304.12 | 304.62 | 305.16 | | 198.01 | 198.11 | 198.39 | 199.26 | |
| 79 | 290.81 | 290.84 | 291.15 | 291.53 | 289. | 185.61 | 185.70 | 185.66 | 186.95 | 184. |
| 80 | 278.57 | 278.59 | 278.86 | 279.12 | | 174.22 | 174.30 | 174.01 | 174.69 | |
| 81 | 267.22 | 267.23 | 267.53 | 267.68 | | 163.72 | 163.79 | 163.30 | 164.12 | |
| 82 | 256.68 | 256.68 | 257.00 | 257.07 | | 154.02 | 154.08 | 153.41 | 154.36 | 153.0 |
| 83 | 246.86 | 246.86 | 247.19 | | | 145.04 | 145.10 | 144.24 | | |
| 84 | 237.69 | 237.68 | | | | 136.71 | 136.76 | | | |
| 85 | 229.12 | 229.11 | 229.51 | | | 128.98 | 129.02 | 127.86 | | |
| 86 | 221.10 | 221.08 | 221.45 | | | 121.77 | 121.81 | 120.51 | | |
| 87 | 213.54 | 213.52 | 213.83 | | | 115.05 | 115.09 | 113.64 | | |
| 88 | 206.43 | 206.40 | 206.60 | | | 108.77 | 108.80 | 107.22 | | |
| 89 | 199.72 | 199.69 | | | | 102.90 | 102.93 | | | |
| 90 | 193.41 | 193.37 | 193.49 | | | 97.40 | 97.43 | 95.62 | | |
| 91 | 187.41 | 187.37 | | | | 92.24 | 92.26 | | | |
| 92 | 181.77 | 181.73 | 181.66 | 181.36 | 175.4 | 87.40 | 87.43 | 85.44 | 87.44 | |
| 93 | 176.39 | 176.34 | | | | 82.85 | 82.87 | | | |
| 94 | 171.32 | 171.31 | | | | 78.58 | 78.60 | | | |
| 95 | 166.47 | 166.46 | | | | 74.55 | 74.57 | | | |
| 96 | 161.88 | 161.88 | | | | 70.75 | 70.77 | | | |
| 97 | 157.50 | 157.49 | | | | 67.17 | 67.19 | | | |
| 98 | 153.36 | 153.35 | | | | 63.80 | 63.81 | | | |
| 99 | 149.41 | 149.40 | | | | 60.61 | 60.63 | | | |
| 100 | 145.65 | 145.64 | | | | 57.60 | 57.61 | | | |

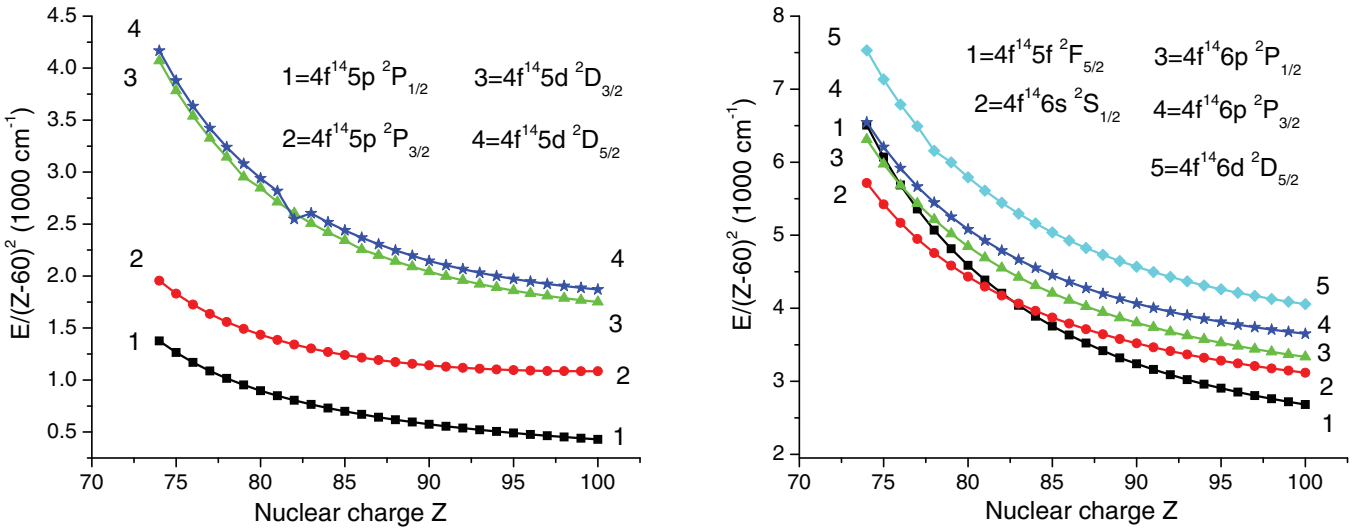


FIG. 1. (Color online) $Z$ dependence of the scaled $4f^{14}nl\ LSJ$ energy levels in Pm-like ions.

approach [5]. The difference between our RMBPT and the MR-MP results for the $4f^{14}5s\ ^2S_{1/2}$-$4f^{14}5p\ ^2P_{3/2}$ transition is larger than for the $4f^{14}5s\ ^2S_{1/2}$-$4f^{14}5p\ ^2P_{1/2}$ transition (0.2%–2.2% and 0.2%–0.7%, respectively).

To explore the cause of such a disagreement, we carried out additional calculations for the wavelengths of Pm-like ions with $Z = 74$–92 using the Hartree-Fock-relativistic method (COWAN code [29]). The following set of configurations was used: $4f^{14}nl$ (with $nl = 5s$, $6s$, $5p$, $6p$, $5d$, $6d$, and $5f$). The core-excited $4f^{13}5s^2$, $4f^{13}5s5p$, $4f^{13}5s5d$, $4f^{13}5s5f$, $4f^{13}5p^2$, $4f^{13}5p5d$, $4f^{12}5s^25p$, $4f^{12}5s^25d$, $4f^{12}5s^25f$, $4f^{12}5s5p^2$, $4f^{12}5s5d^2$, $4f^{12}5s5f^2$, $4f^{12}5s5p5d$, $4f^{12}5s5p5f$, and $4f^{12}5p^3$ configurations were also included in the even- and odd-parity complexes. The results of our calculations are incorporated in Table II in column "COWAN." It should be noted that the scaling of electrostatic integrals in the COWAN code allows us to correct for correlation effects. In many systems it leads to a good agreement with experimental energies. We used the same scaling factor (0.85) for all electrostatic integrals. The 0.85 scaling factor was introduced by Fawcett *et al.* [30]. These authors explained that the 0.85 factor was found empirically to obtain results in good agreement with experiment.

The results given in columns RMBPT and COWAN of Table II are in excellent agreement (0.04%–0.18%) for the $4f^{14}5s\ ^2S_{1/2}$-$4f^{14}5p\ ^2P_{1/2}$ transition except for the results for the ions with $Z = 74$–77, where the difference is 0.5%–1.5%. The largest difference (2.2%) for the $4f^{14}5s\ ^2S_{1/2}$-$4f^{14}5p\ ^2P_{3/2}$ transition is found for the ion with $Z = 92$, while the RMBPT and MR-MP wavelengths are in excellent agreement (0.05%) for Pm-like uranium.

The $4f^{14}nl\ LSJ$ energies, relative to the $4f^{14}5s\ ^2S_{1/2}$ state, divided by $(Z-60)^2$, are shown in Fig. 1. In this figure $Z$ was decreased by 60 to provide a better presentation of the scaled energy. The scaled $4f^{14}nl\ LSJ$ energy is a smooth function of $Z$ for entire interval of $Z = 74$–100, but exhibits irregularities for the $4f^{14}5d\ ^2D_{5/2}$ state at $Z = 82$. These irregularities are caused by exceptionally small energy denominators in the expression for the second-order correlation energy (see for details Ref. [27]). The smallest value of energies are for the $4f^{14}5p\ ^2P_{1/2}$ level (curve 1 in the left panel of Fig. 1). The largest value of energies are for the $4f^{14}6d\ ^2D_{5/2}$ level (curve 5 in the right panel of Fig. 1). Only one curve 1 ($4f^{14}5f\ ^2F_{5/2}$ level) on the right panel of Fig. 1 crosses the curve 3 ($4f^{14}6p\ ^2P_{1/2}$ level) around $Z = 77$ and the curve 2 ($4f^{14}6s\ ^2S_{1/2}$ level) around $Z = 83$.

## III. ENERGIES OF THE $4f$-CORE-EXCITED STATES IN Pm-LIKE IONS

Energies of the $4f$-core-excited states are evaluated using the Hartree-Fock-relativistic method (COWAN code). We obtain our large scale calculations including the following set of configurations: $4f^{14}5s$, $4f^{14}5p$, $4f^{13}5s^2$, $4f^{13}5p^2$, $4f^{13}5s5p$, $4f^{12}5s^25p$, $4f^{12}5s5p^2$, and $4f^{12}5p^3$.

In Fig. 2 we display excitation energies in Pm-like ions for the $4f^{14}5s\ ^2S_{1/2}$ (curve 1), $4f^{13}5s^2\ ^2F_J$ (curves 2 and 3),

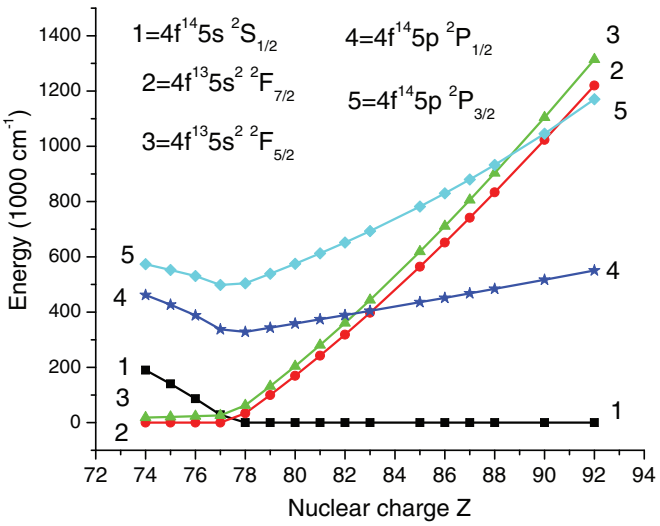


FIG. 2. (Color online) $Z$ dependence of the $4f^{14}5l\ LSJ$ and $4f^{13}5s^2\ LSJ$ energy levels in Pm-like ions.

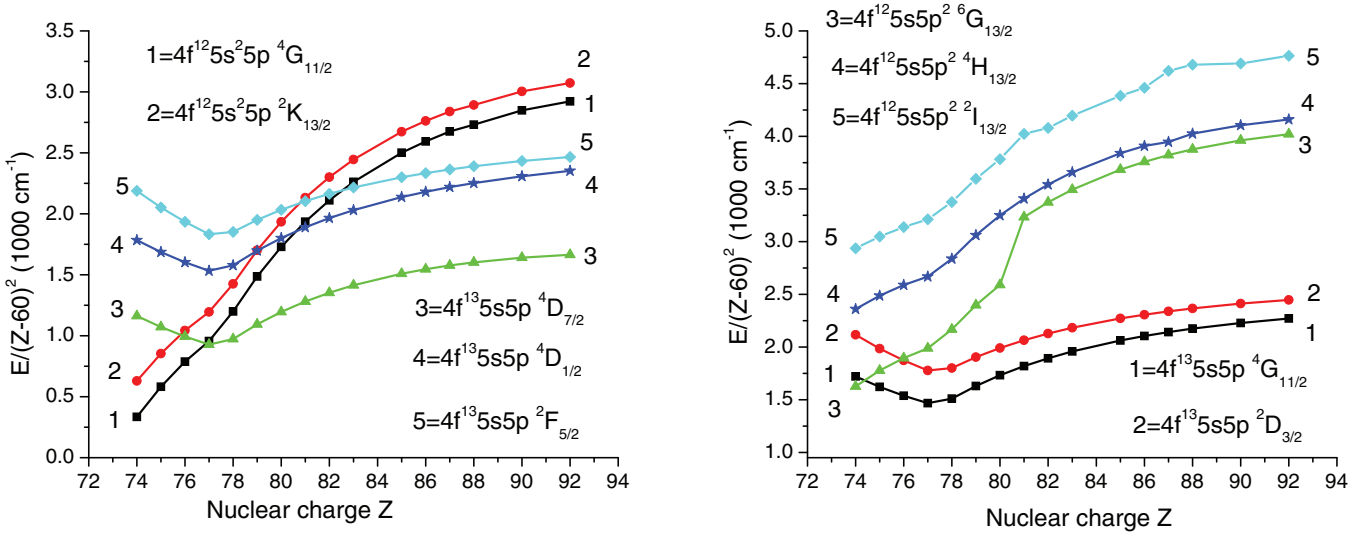


FIG. 3. (Color online) $Z$ dependence of the scaled $4f^{13}5s5p\ LSJ$, $4f^{12}5s^25p\ LSJ$, and $4f^{12}5s5p^2\ LSJ$ energy levels in Pm-like ions.

and $4f^{14}5p\ ^2P_J$ (curves 4 and 5) levels. This figure indicates that the ground state for the Pm-like $W^{13+}$, $Re^{14+}$, $Os^{15+}$, and $Ir^{16+}$ is the $4f^{13}5s^2\ ^2F_{7/2}$ core-excited state (curve 2). The first excited state $4f^{13}5s^2\ ^2F_{5/2}$ was separated from the ground state by 18 600, 20 800, 23 300, and 25 900 $cm^{-1}$ in the $W^{13+}$, $Re^{14+}$, $Os^{15+}$, and $Ir^{16+}$ ions, respectively. The excitation energy of the $4f^{14}5s\ ^2S_{1/2}$ state is almost equal (28 400 $cm^{-1}$) to the energy of the $4f^{13}5s^2\ ^2F_{5/2}$ level for the Pm-like $Ir^{16+}$ ion. For the next Pm-like ion ($Pt^{17+}$), the $4f^{14}5s\ ^2S_{1/2}$ state became the ground state and continues to be the ground state for higher $Z$. Curve 4 describing the energy of the $4f^{14}5p\ ^2P_{1/2}$ level smoothly varies from 461 800 $cm^{-1}$ for $Z = 74$ up to 550 500 $cm^{-1}$ for $Z = 92$ with a minimum at $Z = 78$. Curves 2 and 3 describing the $4f^{13}5s^2\ ^2F_J$ energies cross curve 4 around $Z = 83$. Curve 5 describing the energy of the $4f^{14}5p\ ^2P_{3/2}$ level crosses the curves 2 and 3 around $Z = 90$.

A limited number of $4f^{13}5s5p\ LSJ$, $4f^{12}5s^25p\ LSJ$, and $4f^{12}5s5p^2\ LSJ$ energy levels is illustrated in Fig. 3. For better presentation we again display the excitation energies divided by $(Z-60)^2$. The left panel of Fig. 3 displays the scaled energy levels due to configurations $4f^{13}5s5p\ LSJ$ and $4f^{12}5s^25p\ LSJ$. Curves 1 and 2, describing energies of the $4f^{12}5s^25p\ ^4G_{11/2}$ and $4f^{12}5s^25p\ ^2K_{13/2}$ levels, cross curves 3, 4, and 5, describing energies of the $4f^{13}5s5p\ LSJ$ levels with $LSJ = {}^4D_{7/2}$, $^4D_{1/2}$, and $^2F_{5/2}$, respectively. The difference in energies near the crossing points becomes very small (1%–3% of the total energy). The difference between the energies of the $4f^{12}5s^25p\ ^2K_{13/2}$ and $4f^{13}5s5p\ ^4D_{1/2}$ levels at $Z = 79$ is equal to 800 $cm^{-1}$; that corresponds to 0.12% of the 613 900 and 613 100cm $^{-1}$ energies of these levels, respectively. To the best of our knowledge, crossing of levels attributed to configurations with a different number of $4f$ electrons ($4f^{13}5s5p\ LSJ$ and $4f^{12}5s^25p\ LSJ$) was never discussed in a publication before.

The distribution of energy levels of the $4f^{13}5s5p$ and $4f^{12}5s5p^2$ configurations is illustrated in the right panel of Fig. 3. From this figure it is evident that the energies of the $4f^{12}5s5p^2\ LSJ$ levels are larger than the energies of the $4f^{13}5s5p\ LSJ$ levels. Only two crossings take place between the $4f^{12}5s5p^2\ ^6G_{13/2}$ and $4f^{13}5s5p\ LSJ$ with $LSJ = {}^4G_{11/2}$ and $^2D_{3/2}$ at $Z = 74$ and $Z = 77$, respectively. The energy difference between the $4f^{12}5s5p^2\ ^6G_{13/2}$ and $4f^{13}5s5p\ ^2D_{3/2}$, described by the curves 3 and 2 is equal to 5700 $cm^{-1}$; that corresponds to 1.2% of these respected energies of 479 500 and 485 200 $cm^{-1}$.

## IV. ENERGIES AND LIFETIMES IN THE Pm-LIKE $W^{13+}$ ION

In Tables III and IV the energies, lifetimes, and sums of radiative decays of the excited levels in Pm-like $W^{13+}$ ion are displayed. Energies are given relative to the $4f^{13}5s^2\ ^2F_{7/2}$ ground state. In Table III we list the results obtained for the even-parity $4f^{14}5s\ ^2S_{1/2}$, $4f^{13}5s5p\ LSJ$, $4f^{12}5s5p^2\ LSJ$, $4f^{11}5s5p^3\ LSJ$, and $4f^{10}5s5p^4\ LSJ$ states. The results for the odd-parity $4f^{14}5p\ ^2P_J$, $4f^{13}5p^2\ LSJ$, $4f^{12}5s^25p\ LSJ$, $4f^{12}5p^3\ LSJ$, $4f^{11}5s^25p^2\ LSJ$, and $4f^{10}5s^25p^3\ LSJ$ states are given in Table IV. Our large-scale calculations of atomic properties are based on the previously mentioned code developed by COWAN, which uses a quasirelativistic Hartree-Fock method with superposition of configurations (COWAN code) [29,31]. With almost 4000 levels per parity, the total number of radiative transitions is millions. To reduce the computational load, we neglected transitions with small probabilities, $gA_r < 10^5\ s^{-1}$ (the strongest transitions, as will be shown below, have $A_r$ on the order of $10^{14}\ s^{-1}$). Even with this restriction, the resulting list of radiative transitions within the Pm-like $W^{13+}$ ion includes about 532 000 transitions.

We reorganize this file by order of energies to evaluate the sum of radiative decays $\Sigma A_r$ and lifetime values as $\frac{1}{\sum A_r} = \tau$ for the 7815 levels from the $4f^{14}5s$, $4f^{14}5p$, $4f^{13}5s^2$, $4f^{13}5s5p$, $4f^{13}5p^2$, $4f^{12}5s^25p$, $4f^{12}5s5p^2$, $4f^{12}5p^3$, $4f^{11}5s^25p^2$, $4f^{11}5s5p^3$, $4f^{10}5s^25p^3$, and $4f^{10}5s5p^4$ configurations. We only considered electric dipole transitions and did not evaluate lifetimes for metastable levels, such as the $4f^{13}5s^2\ ^2F_{5/2}$ level.

TABLE III. Energies ($cm^{-1}$), lifetimes ($10^{-10}$ s), and sums of radiative decays $\sum A_r$ ($s^{-1}$) for even parity levels in Pm-like $W^{13+}$ ion. Energies are given relative to the $4f^{13}5s^2\ ^2F_{7/2}$ ground state. We use intermediate and level $(^{2S_0+1}L_0)\ ^{2S+1}L_J$ designation. The upper indices are used in the COWAN code to differentiate between atomic terms.

| Level | Energy $10^3$ $cm^{-1}$ | Lifetime $10^{-10}$ s | $\sum A_r$ $s^{-1}$ | Level | Energy $10^3$ $cm^{-1}$ | Lifetime $10^{-10}$ s | $\sum A_r$ $s^{-1}$ |
|---|---|---|---|---|---|---|---|
| | $4f^{14}5s$ configuration | | | | $4f^{12}5s5p^2$ configuration | | |
| $(^1S)\ ^2S_{1/2}$ | 197.100 | 63010 | 1.59[05] | $(^3H)\ ^6G_{13/2}$ | 325.410 | 2.325 | 4.30[09] |
| | $4f^{13}5s5p$ configuration | | | $(^3H)\ ^6H_{11/2}$ | 332.679 | 2.260 | 4.43[09] |
| $(^2F)\ ^4D_{7/2}$ | 234.175 | 100.6 | 9.94[07] | $(^3F)\ ^6D_{9/2}$ | 334.414 | 2.312 | 4.33[09] |
| $(^2F)\ ^4D_{7/2}$ | 249.219 | 5.203 | 1.92[09] | $(^1G)\ ^4H_{7/2}$ | 339.330 | 2.208 | 4.53[09] |
| $(^2F)\ ^4G_{5/2}$ | 251.344 | 8.934 | 1.12[09] | $(^3H)\ ^6I_{9/2}$ | 347.331 | 2.336 | 4.28[09] |
| $(^2F)\ ^4G_{9/2}$ | 251.793 | 3.729 | 2.68[09] | $(^3F)\ ^6G_{3/2}$ | 351.791 | 2.363 | 4.23[09] |
| $(^2F)\ ^4G_{5/2}$ | 257.575 | 4.801 | 2.08[09] | $(^3F)\ ^6G_{5/2}$ | 352.166 | 2.592 | 3.86[09] |
| $(^2F)\ ^2D^a_{5/2}$ | 271.559 | 4.797 | 2.09[09] | $(^3H)\ ^2H^d_{11/2}$ | 352.618 | 1.925 | 5.19[09] |
| $(^2F)\ ^2G^a_{7/2}$ | 273.150 | 3.574 | 2.80[09] | $(^3H)\ ^6I_{7/2}$ | 353.459 | 2.310 | 4.33[09] |
| $(^2F)\ ^4F_{3/2}$ | 274.677 | 3.428 | 2.92[09] | $(^1G)\ ^4G_{9/2}$ | 359.149 | 2.109 | 4.74[09] |
| $(^2F)\ ^4G_{11/2}$ | 343.567 | 290.5 | 3.44[07] | $(^3F)\ ^2F^d_{7/2}$ | 362.061 | 2.035 | 4.91[09] |
| $(^2F)\ ^4D_{3/2}$ | 350.154 | 91280 | 1.10[05] | $(^3F)\ ^4G^a_{5/2}$ | 363.176 | 2.038 | 4.91[09] |
| $(^2F)\ ^4D_{3/2}$ | 350.154 | 80.98 | 1.24[08] | $(^1G)\ ^4H_{7/2}$ | 374.890 | 2.122 | 4.71[09] |
| $(^2F)\ ^4D_{5/2}$ | 352.562 | 11.06 | 9.04[08] | $(^3P)\ ^6P_{5/2}$ | 377.746 | 2.147 | 4.66[09] |
| $(^2F)\ ^4F_{7/2}$ | 355.728 | 23.45 | 4.26[08] | $(^3F)\ ^6G_{3/2}$ | 378.361 | 2.207 | 4.53[09] |
| $(^2F)\ ^4F_{9/2}$ | 355.870 | 35.56 | 2.81[08] | $(^3H)\ ^4I^a_{9/2}$ | 379.226 | 1.986 | 5.04[09] |
| $(^2F)\ ^4D_{1/2}$ | 355.938 | 264.4 | 3.78[07] | $(^3P)\ ^6D_{1/2}$ | 380.634 | 2.478 | 4.04[09] |
| $(^2F)\ ^4F_{3/2}$ | 367.178 | 19.77 | 5.06[08] | $(^1I)\ ^4I_{13/2}$ | 387.288 | 2.166 | 4.62[09] |
| $(^2F)\ ^2G^a_{9/2}$ | 368.935 | 24.07 | 4.16[08] | $(^1I)\ ^4K_{11/2}$ | 387.468 | 2.140 | 4.67[09] |
| $(^2F)\ ^4F_{5/2}$ | 374.366 | 30.60 | 3.27[08] | $(^3P)\ ^6D_{3/2}$ | 388.081 | 2.277 | 4.39[09] |
| $(^2F)\ ^4F_{7/2}$ | 375.741 | 13.12 | 7.62[08] | $(^1D)\ ^4F_{5/2}$ | 397.891 | 2.176 | 4.59[09] |
| $(^2F)\ ^2D^b_{5/2}$ | 404.927 | 0.153 | 6.55[10] | $(^3P)\ ^4D^a_{1/2}$ | 400.282 | 1.815 | 5.51[09] |
| $(^2F)\ ^2G^b_{9/2}$ | 405.923 | 0.148 | 6.73[10] | $(^3H)\ ^6H_{15/2}$ | 404.877 | 19.12 | 5.23[08] |
| $(^2F)\ ^2F^b_{7/2}$ | 415.586 | 0.138 | 7.23[10] | $(^3P)\ ^2D^a_{3/2}$ | 404.917 | 1.878 | 5.32[09] |
| $(^2F)\ ^2D^b_{3/2}$ | 420.946 | 0.153 | 6.52[10] | $(^3F)\ ^6G_{11/2}$ | 416.157 | 10.86 | 9.21[08] |
| $(^2F)\ ^2G^b_{7/2}$ | 425.595 | 0.191 | 5.24[10] | $(^3F)\ ^6D_{9/2}$ | 418.963 | 11.85 | 8.44[08] |
| $(^2F)\ ^2F^b_{5/2}$ | 435.197 | 0.138 | 7.25[10] | $(^3H)\ ^6G_{9/2}$ | 422.620 | 9.354 | 1.07[09] |
| | $4f^{11}5s5p^3$ configuration | | | | $4f^{10}5s5p^4$ configuration | | |
| $(^4I)\ ^8I_{19/2}$ | 541.575 | 2.050 | 4.88[09] | $(^5I)\ ^8K_{21/2}$ | 844.523 | 0.385 | 2.60[10] |
| $(^4I)\ ^8I_{17/2}$ | 548.184 | 1.054 | 9.49[09] | $(^5I)\ ^8I_{19/2}$ | 851.511 | 0.383 | 2.61[10] |
| $(^4I)\ ^8I_{15/2}$ | 553.025 | 1.634 | 6.12[09] | $(^5I)\ ^8I_{17/2}$ | 857.098 | 0.373 | 2.68[10] |
| $(^4I)\ ^8I_{13/2}$ | 558.002 | 1.216 | 8.23[09] | $(^5I)\ ^8I_{15/2}$ | 862.724 | 0.366 | 2.73[10] |
| $(^4I)\ ^8I_{11/2}$ | 562.606 | 0.568 | 1.76[10] | $(^5I)\ ^8H_{13/2}$ | 868.789 | 0.416 | 2.40[10] |
| $(^4F)\ ^8F_{13/2}$ | 566.711 | 1.761 | 5.68[09] | $(^5I)\ ^8K_{19/2}$ | 870.004 | 0.348 | 2.88[10] |
| $(^4I)\ ^8I_{9/2}$ | 567.044 | 1.716 | 5.83[09] | $(^5I)\ ^8I_{15/2}$ | 870.245 | 0.375 | 2.66[10] |
| $(^2H)\ ^6H^d_{15/2}$ | 568.720 | 1.605 | 6.23[09] | $(^5I)\ ^8K_{17/2}$ | 870.381 | 0.360 | 2.78[10] |
| $(^4I)\ ^6I^b_{17/2}$ | 568.927 | 1.375 | 7.27[09] | $(^5I)\ ^8I_{13/2}$ | 873.324 | 0.646 | 1.55[10] |
| $(^4I)\ ^8I_{7/2}$ | 569.424 | 0.938 | 1.07[10] | $(^5F)\ ^8G_{15/2}$ | 875.505 | 0.373 | 2.68[10] |

Most of the odd-parity $4f^{12}5s^25p$ $LSJ$ levels are metastable. The energies of the 69 levels of the odd-parity $4f^{12}5s^25p$ $LSJ$ states are distributed in the region between 68 400 and 312 600 $cm^{-1}$. Only the $4f^{14}5s\ ^2S_{1/2}$-$4f^{12}5s^25p(^1D)\ ^2P_{1/2}$ and $4f^{14}5s\ ^2S_{1/2}$-$4f^{12}5s^25p(^1S)\ ^2P_{3/2}$ electric-dipole transitions contribute to the lifetime of the $4f^{12}5s^25p(^1D)\ ^2P_{1/2}$ and $4f^{12}5s^25p(^1S)\ ^2P_{3/2}$ levels, respectively. The lifetime of these two levels are given in the right column of Table IV. The above mentioned transitions are the two-electron $4f^2$-$5s5p$ transitions with transition rates $A_r$ equal to $1.22 \times 10^5$ and $3.83 \times 10^5$ $s^{-1}$. We already mentioned that the COWAN code we used displays transitions with $gA_r > 10^5$ $s^{-1}$. This is why we did not find out the other two electron $4f^2$-$5s5p$ transitions with $gA_r < 10^5$ $s^{-1}$. Those two electron transitions have nonzero $A_r$ values due to small mixing inside the even-parity $4f^{14}5s + 4f^{12}5s5p^2$ complex as well as the odd-parity $4f^{12}5s^25p + 4f^{14}5p$ complex.

The same mixing inside the even-parity and odd-parity complexes is responsible for the nonzero value of the lifetime of the $4f^{14}5s\ ^2S_{1/2}$ level. The $A_r$ values for the $4f^{12}5s^25p(^3F)\ ^4F_{3/2}$-$4f^{14}5s\ ^2S_{1/2}$ and $4f^{12}5s^25p(^1D)\ ^2D_{3/2}$-$4f^{14}5s\ ^2S_{1/2}$ transitions are equal to $0.979 \times 10^5$ and $0.608 \times 10^5$ $s^{-1}$, respectively. That gives us the values of the $\Sigma A_r$ and lifetime for the $4f^{14}5s\ ^2S_{1/2}$ level listed in the left column of Table III.

The next odd-parity $4f^{11}5s^25p^2$ $LSJ$ levels are distributed in the region between 184 600 and 639 200 $cm^{-1}$. The lifetimes of the 15 $4f^{11}5s^25p^2$ $LSJ$ low-lying levels (among

TABLE IV. Energies ($cm^{-1}$), lifetimes ($10^{-10}$ and $10^{-5}$ s), and sums of radiative decays $\sum A_r$ ($s^{-1}$) for odd-parity levels in Pm-like $W^{13+}$ ion. Energies are given relative to the $4f^{13}5s^2\ ^2F_{7/2}$ ground state. We use intermediate and level $(^{2S_0+1}L_0)\ ^{2S+1}L_J$ designation. The upper indices are used in the COWAN code to differentiate between atomic terms.

| Level | Energy $10^3$ $cm^{-1}$ | Lifetime $10^{-10}$ s | $\sum A_r$ $s^{-1}$ | Level | Energy $10^3$ $cm^{-1}$ | Lifetime $10^{-5}$ s | $\sum A_r$ $s^{-1}$ |
|---|---|---|---|---|---|---|---|
| | $4f^{14}5p$ configuration | | | | $4f^{12}5s^25p$ configuration | | |
| $(^1S)\ ^2P_{1/2}$ | 467.041 | 0.740 | 1.35[10] | $(^1D)\ ^2P_{1/2}$ | 271.041 | 0.818 | 1.22[05] |
| $(^1S)\ ^2P_{3/2}$ | 577.405 | 0.267 | 3.75[10] | $(^1S)\ ^2P_{3/2}$ | 312.559 | 0.261 | 3.83[05] |
| | $4f^{13}5p^2$ configuration | | | | $4f^{11}5s^25p^2$ configuration | | |
| $(^3P)\ ^4F_{7/2}$ | 547.893 | 0.270 | 3.70[10] | $(^2F)\ ^4G^d_{5/2}$ | 333.010 | 1.382 | 7.24[04] |
| $(^3P)\ ^4G_{5/2}$ | 569.101 | 0.265 | 3.77[10] | $(^4S)\ ^4D_{5/2}$ | 334.256 | 5.676 | 1.76[04] |
| $(^3P)\ ^4F_{9/2}$ | 640.812 | 0.163 | 6.15[10] | $(^4F)\ ^4F^b_{7/2}$ | 341.924 | 7.692 | 1.30[04] |
| $(^3P)\ ^2F_{5/2}$ | 646.441 | 0.160 | 6.26[10] | $(^4F)\ ^2F_{7/2}$ | 345.314 | 0.464 | 2.16[05] |
| $(^3P)\ ^2G_{7/2}$ | 652.129 | 0.155 | 6.46[10] | $(^4G)\ ^6F_{7/2}$ | 347.602 | 0.861 | 1.16[05] |
| $(^3P)\ ^4F_{3/2}$ | 653.571 | 0.173 | 5.77[10] | $(^4G)\ ^4G^a_{9/2}$ | 348.172 | 4.537 | 2.20[04] |
| $(^1D)\ ^2H_{11/2}$ | 655.801 | 0.220 | 4.55[10] | $(^2D)\ ^4P1_{5/2}$ | 349.051 | 5.698 | 1.76[04] |
| $(^1D)\ ^2D_{5/2}$ | 658.983 | 0.203 | 4.92[10] | $(^4F)\ ^4H_{7/2}$ | 351.159 | 5.571 | 1.80[04] |
| $(^1D)\ ^2P_{3/2}$ | 660.027 | 0.201 | 4.97[10] | $(^4F)\ ^4H_{9/2}$ | 352.651 | 2.632 | 3.80[04] |
| $(^1D)\ ^2F_{7/2}$ | 662.596 | 0.192 | 5.22[10] | $(^4G)\ ^6H_{7/2}$ | 353.239 | 5.188 | 1.93[04] |
| $(^1D)\ ^2G_{9/2}$ | 664.983 | 0.180 | 5.55[10] | $(^4F)\ ^4F^a_{7/2}$ | 356.303 | 1.950 | 5.13[04] |
| $(^3P)\ ^4G_{7/2}$ | 667.338 | 0.159 | 6.27[10] | $(^4I)\ ^4K^b_{11/2}$ | 358.040 | 7.130 | 1.40[04] |
| $(^3P)\ ^4G_{5/2}$ | 670.902 | 0.158 | 6.35[10] | $(^4G)\ ^4H^a_{7/2}$ | 359.910 | 5.626 | 1.78[04] |
| $(^1D)\ ^2P_{1/2}$ | 672.732 | 0.214 | 4.67[10] | $(^4G)\ ^6G_{3/2}$ | 360.155 | 3.162 | 3.16[04] |
| $(^1D)\ ^2H_{9/2}$ | 675.352 | 0.207 | 4.84[10] | $(^4G)\ ^4F^b_{9/2}$ | 362.176 | 1.779 | 5.62[04] |
| | $4f^{12}5p^3$ configuration | | | | $4f^{10}5s^25p^3$ configuration | | |
| $(^3H)\ ^4I^b_{15/2}$ | 760.147 | 0.118 | 8.48[10] | $(^5I)\ ^8I_{15/2}$ | 470.871 | 2.636 | 3.79[04] |
| $(^3H)\ ^4H^a_{11/}$ | 766.303 | 0.122 | 8.17[10] | $(^5I)\ ^4H^b_{13/2}$ | 477.519 | 4.447 | 2.25[04] |
| $(^3H)\ ^2G^b_{9/2}$ | 767.703 | 0.125 | 8.00[10] | $(^5I)\ ^8I_{15/2}$ | 482.486 | 7.820 | 1.28[04] |
| $(^3H)\ ^4H_{13/2}$ | 771.067 | 0.222 | 4.50[10] | $(^5I)\ ^8I_{13/2}$ | 483.544 | 4.031 | 2.48[04] |
| $(^3F)\ ^4F_{9/2}$ | 772.274 | 0.124 | 8.06[10] | $(^5I)\ ^8I_{11/2}$ | 486.033 | 4.213 | 2.37[04] |
| $(^3H)\ ^4G^b_{7/2}$ | 775.579 | 0.131 | 7.66[10] | $(^5F)\ ^6G^b_{13/2}$ | 487.372 | 4.118 | 2.43[04] |
| $(^1G)\ ^2F^b_{5/2}$ | 776.984 | 0.119 | 8.38[10] | $(^5I)\ ^8I_{9/2}$ | 491.019 | 1.719 | 5.82[04] |
| $(^3F)\ ^6F_{11/2}$ | 777.247 | 0.119 | 8.42[10] | $(^5I)\ ^4K^b_{15/2}$ | 493.551 | 0.933 | 1.07[05] |
| $(^3H)\ ^4G^b_{7/2}$ | 781.944 | 0.122 | 8.22[10] | $(^5I)\ ^4I_{13/2}$ | 494.533 | 3.772 | 2.65[04] |
| $(^3H)\ ^4I^b_{13/2}$ | 782.954 | 0.136 | 7.34[10] | $(^5I)\ ^8I_{7/2}$ | 495.722 | 1.678 | 5.96[04] |
| $(^3F)\ ^6F_{5/2}$ | 786.667 | 0.121 | 8.29[10] | $(^5I)\ ^4H^b_{11/2}$ | 496.470 | 1.419 | 7.05[04] |
| $(^3H)\ ^6H_{9/2}$ | 787.211 | 0.119 | 8.37[10] | $(^5I)\ ^8I_{5/2}$ | 497.554 | 3.812 | 2.62[04] |
| $(^3F)\ ^6F_{3/2}$ | 790.322 | 0.121 | 8.26[10] | $(^5F)\ ^6G^b_{11/2}$ | 499.146 | 1.742 | 5.74[04] |
| $(^3H)\ ^6H_{11/2}$ | 790.777 | 0.118 | 8.48[10] | $(^5F)\ ^8F_{5/2}$ | 499.676 | 3.423 | 2.92[04] |
| $(^3F)\ ^6F_{7/2}$ | 792.827 | 0.118 | 8.46[10] | $(^5I)\ ^4K^b_{13/2}$ | 501.864 | 2.189 | 4.57[04] |

590 levels) displayed in the right column of Table IV are obtained mostly from the $4f^{13}5s5p\ L'S'J'$-$4f^{11}5s^25p^2\ LSJ$ transitions. Those transitions are again two-electron $4f^2$-$5s5p$ transitions. We can see from the right column of Table IV that the lifetimes of these levels is about $10^{-5}$ s.

The odd-parity $4f^{10}5s^25p^3\ LSJ$ levels (about 2900 levels) are distributed in the region between 463 100 and 1 028 000 $cm^{-1}$. The same two-electron $4f^2$-$5s5p$ transitions are responsible for the lifetime values of the odd-parity $4f^{10}5s^25p^3\ LSJ$ levels. Energies, lifetimes, and sums of radiative decays for the 15 low-lying levels are displayed in the right column of Table IV.

The dominant contribution in the lifetime of the $4f^{14}5p\ ^2P_J$ levels is from the $4f^{14}5s\ ^2S_{1/2}$-$4f^{14}5p\ ^2P_J$ transitions. Results are displayed in the left column of Table IV. The contribution of the $4f^{13}5s5p\ LSJ$-$4f^{14}5p\ ^2P_J$ transitions is less than 1% in the $4f^{14}5p\ ^2P_J$ lifetime. The $A_r$ values of the $4f^{12}5s5p^2\ LSJ$-$4f^{14}5p\ ^2P_J$ transition is less than $4f^{14}5s\ ^2S_{1/2}$-$4f^{14}5p\ ^2P_J$ transitions by five orders of magnitude. Such a large contribution by the $4f^{14}5s\ ^2S_{1/2}$-$4f^{14}5p\ ^2P_J$ transitions to the $4f^{14}5p\ ^2P_J$ lifetimes is due to the importance of the $5s$-$5p$ one-electron dipole transition compared with the $5s$-$4f$ one-electron octupole or the $5s5p$-$4f^2$ two-electron transition.

The $5s$-$5p$ one-electron dipole transition gives the dominant contribution to the lifetimes of the even-parity $4f^{13}5s5p\ LSJ$, $4f^{12}5s5p^2\ LSJ$, $4f^{11}5s5p^3\ LSJ$, and $4f^{10}5s5p^4\ LSJ$ states. In Table III we list energies, lifetimes, and sum of radiative decays in Pm-like $W^{13+}$ ion for the low-lying levels of these configurations.

The $4f^{13}5s5p\ L'S'J'$-$4f^{13}5p^2\ LSJ$ transitions are the dominant transitions in the determination of the $4f^{13}5p^2\ LSJ$ lifetime values. Results for the 15 levels are listed in the left column of Table IV. In order to determine the

lifetime of the $4f^{12}5p^3$ $LSJ$ lifetime, we consider 67 510 transitions, including the $4f^{12}5s5p^2$ $L'S'J'$-$4f^{12}5p^3$ $LSJ$ and $4f^{11}5s5p^3$ $L'S'J'$-$4f^{12}5p^3$ $LSJ$ transitions. Energies, lifetimes, and sum of radiative decays for the 15 $4f^{12}5p^3$ $LSJ$ low-lying levels are presented the left column of Table IV.

We have tried to compare our lifetimes values listed in Tables III and IV with lifetime values given by Vilkas *et al*. [5]. Unfortunately, only occupation numbers were given for labeling levels instead of configurations and terms as are usually used for the identification of levels. Only three levels were identified as $4f^{14}5s\ ^2S_{1/2}$, $4f^{14}5p\ ^2P_{1/2}$, and $4f^{14}5p\ ^2S_{3/2}$. However, values of the energy and lifetime were presented only for the $4f^{14}5s\ ^2S_{1/2}$ level. We find a substantial difference in energies (197 100 vs 177 727 $cm^{-1}$) and lifetimes ($0.630 \times 10^{-5}$ vs $1.165 \times 10^{-5}$ s). It is rather strange to find such large difference in the energy of the $4f^{14}5s\ ^2S_{1/2}$ level since there is less than 1% disagreement in the wavelengths of the $4f^{14}5s\ ^2S_{1/2}$-$4f^{14}5p\ ^2P_{1/2}$ and $4f^{14}5s\ ^2S_{1/2}$-$4f^{14}5p\ ^2P_{3/2}$ transitions (Table II).

## V. WAVELENGTHS AND TRANSITIONS IN Pm-LIKE $W^{13+}$ AND $Au^{18+}$ IONS

In Table V we display a short list of transitions from the ground state in Pm-like $W^{13+}$ and $Au^{18+}$ ions. We choose these ions as an example to illustrate our results for the Pm-like sequence because they have a different ground state; the $4f^{13}5s^2\ ^2F_{7/2}$ level for ions with $Z = 74$–77, and the $4f^{14}5s\ ^2S_{1/2}$ level for ions with $Z = 78$–100. To check the accuracy of our calculations, we evaluated radiative transition rates and wavelengths in Pm-like $W^{13+}$ and $Au^{18+}$ ions using the COWAN and HULLAC codes. About 430 energy levels are found for the set of six $4f^{14}5s$, $4f^{14}5p$, $4f^{13}5s^2$, $4f^{13}5s5p$, $4f^{12}5s^25p$, and $4f^{12}5s5p^2$ configurations. There are 180 transitions from the $4f^{13}5s^2\ ^2F_{7/2}$ level in Pm-like $W^{13+}$ ion and only 18 transitions from the $4f^{14}5s\ ^2S_{1/2}$ level in Pm-like $Au^{18+}$ ion.

In Table V we list wavelengths and weighted transition rates for the $4f^{13}5s^2\ ^2F_{7/2}$-$4f^{13}5s5p$ $LSJ$ and $4f^{13}5s^2\ ^2F_{7/2}$-$4f^{12}5s5p^2$ $LSJ$ transitions in the Pm-like $W^{13+}$ ion, as well as for the $4f^{14}5s\ ^2S_{1/2}$-$4f^{14}5p$ $LSJ$ and $4f^{14}5s\ ^2S_{1/2}$-$4f^{12}5s^25p$ $LSJ$ transitions in Pm-like $Au^{18+}$ ion. In the left column of Table V we use the designations of levels used in the COWAN code: configuration, intermediate, and level $(^{2S_0+1}L_0)\ ^{2S+1}L_J$ designation. The upper indices are used in the COWAN code to differentiate between atomic terms. The labeling of a level is chosen by the largest mixing coefficient in a given complex with fixed $J$ and parity. In the HULLAC code, a level's name has 12 characters, the first four are the name of the parent nonrelativistic configuration given in the input file, the next two digits represent the specific relativistic subconfiguration, the next four represent part of the recoupling scheme used, and the last two are the twice the total $J$ value of the level. The level's name is unique, i.e., for the same definition of configuration the same level name will be used in the final result.

A comparison of the wavelength values given in columns COWAN and HULLAC of Table V demonstrates good agreement (0.2%–1.0%) for most transitions; exceptions are the $4f^{14}5s\ ^2S_{1/2}$-$4f^{12}5s^25p\ (^3P)\ ^4D_{1/2}$ and

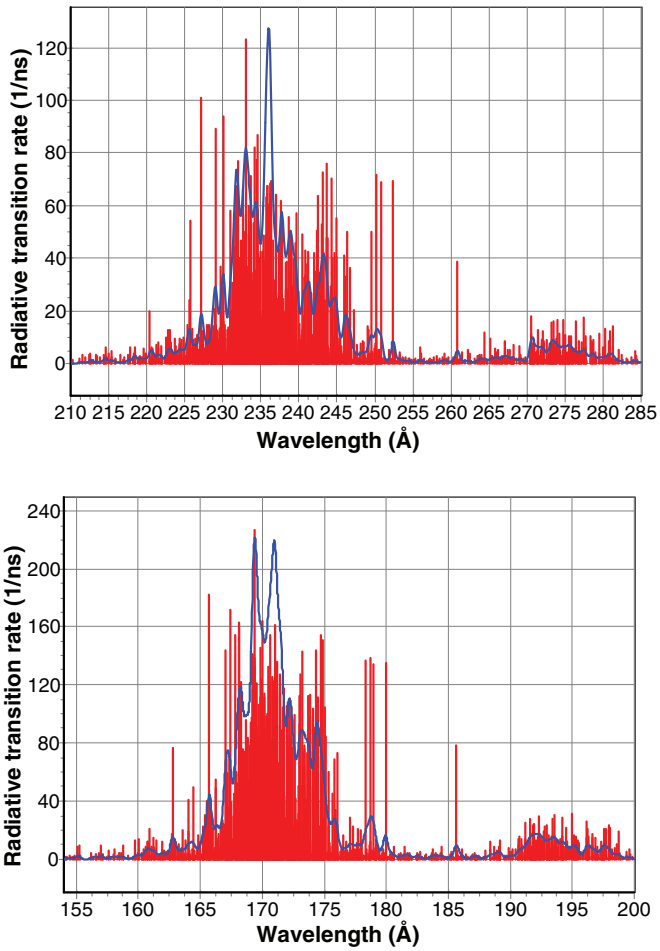


FIG. 4. (Color online) Synthetic spectra (red) for the $[4f^{14}5s + 4f^{13}5s5p + 4f^{12}5s5p^2] \leftrightarrow [4f^{14}5p + 4f^{13}5s^2 + 4f^{12}5s^25p]$ transitions in Pm-like $W^{13+}$ (top) and Pm-like $Au^{18+}$ (bottom). A resolving power $R = E/\Delta E = 400$ is assumed to produce a Gaussian profile (blue).

$4f^{14}5s\ ^2S_{1/2}$-$4f^{12}5s^25p\ (^3P)\ ^2P_{1/2}$ transitions where the difference is about 1.9%. The difference in the weighted transition rates $gA_r$ displayed in columns COWAN and HULLAC of Table V is about 2%–20% for most transitions; exceptions are the $4f^{14}5s\ ^2S_{1/2}$-$4f^{12}5s^25p\ (^1S)\ ^2P_{1/2}$ and $4f^{14}5s\ ^2S_{1/2}$-$4f^{12}5s^25p\ (^3P)\ ^2P_{1/2}$ transitions where the difference is about 30%. These transitions are the $4f^2$-$5s5p$ two-electron transitions with nonzero values of $gA_r$ only due to mixing inside of their complexes.

Synthetic spectra for the Pm-like $W^{13+}$ ion and the Pm-like $Au^{18+}$ ion are presented in the upper and lower panels, respectively, of Fig. 4. It was assumed that spectral lines have intensities proportional to the associated radiative transition probabilities. All lines are convolved with a Gaussian profile. Both spectra include about 2000 transitions between even-parity $[4f^{14}5s + 4f^{13}5s5p + 4f^{12}5s5p^2]$ and odd-parity $[4f^{14}5p + 4f^{13}5s^2 + 4f^{12}5s^25p]$ complexes.

Specifically, the spectrum of Pm-like $W^{13+}$ covers the spectral region between 150 and 440 Å, but only the part of the spectrum between 210 and 265 Å is displayed in the upper half of Fig 4. Lines with a small $A_r$ value less than 10 (in units of $10^9$ $s^{-1}$) were omitted. The most intense peaks at

TABLE V. Wavelengths (λ in Å) and weighted transition rates ($gA_r$ in 1/s) for transitions from the $4f^{13}5s^2\ ^2F_{7/2}$ ground state in Pm-like $W^{13+}$ and for transitions from the $4f^{14}5s\ ^2S_{1/2}$ ground state in Pm-like $Au^{18+}$ ions evaluated by the COWAN and HULLAC codes.

| Level | Wavelengths (λ in Å) | | Transition rates ($gA_r$ in 1/s) | | Level |
|---|---|---|---|---|---|
| COWAN | COWAN | HULLAC | COWAN | HULLAC | HULLAC |
| | $4f^{13}5s^2\ ^2F_{7/2}$-$4f^{13}5s5p$ $LSJ$ transitions in Pm-like $W^{13+}$ ion | | | | |
| $4f^{13}5s5p(^2F)\ ^4D_{7/2}$ | 402.084 | 403.040 | 1.48[10] | 1.79[10] | $f13sp$ 0303..07 |
| $4f^{13}5s5p(^2F)\ ^2G^a_{9/2}$ | 271.361 | 272.130 | 3.59[09] | 4.18[09] | $f13sp$ 0008..09 |
| $4f^{13}5s5p(^2F)\ ^4F_{5/2}$ | 267.402 | 267.413 | 1.38[09] | 1.28[09] | $f13sp$ 0004..05 |
| | $4f^{13}5s^2\ ^2F_{7/2}$-$4f^{12}5s5p^2$ $LSJ$ transitions in Pm-like $W^{13+}$ ion | | | | |
| $4f^{12}5s5p^2\ (^1G)\ ^4F_{5/2}$ | 220.495 | 223.289 | 4.42[08] | 5.06[08] | $f12sp2$ 0409..05 |
| $4f^{12}5s5p^2\ (^3H)\ ^4F_{5/2}$ | 214.114 | 218.466 | 1.24[09] | 1.47[09] | $f12sp2$ 041$n$..05 |
| $4f^{12}5s5p^2\ (^3F)\ ^2F^a_{7/2}$ | 210.105 | 210.977 | 1.70[08] | 1.80[08] | $f12sp2$ 040$o$..07 |
| $4f^{12}5s5p^2\ (^3P)\ ^4D_{7/2}$ | 205.109 | 207.079 | 3.14[08] | 2.83[08] | $f12sp2$ 050$t$..07 |
| $4f^{12}5s5p^2\ (^3H)\ ^4H^b_{9/2}$ | 192.033 | 191.837 | 2.92[08] | 3.00[08] | $f12sp2$ 041$i$..09 |
| $4f^{12}5s5p^2\ (^3P)\ ^2F_{7/2}$ | 185.109 | 184.707 | 3.93[07] | 4.06[07] | $f12sp2$ 030$o$..07 |
| $4f^{12}5s5p^2\ (^1G)\ ^2F^b_{5/2}$ | 167.316 | 168.920 | 9.86[06] | 8.16[06] | $f12sp2$ 000$j$..05 |
| $4f^{12}5s5p^2\ (^3H)\ ^4G^b_{9/2}$ | 155.915 | 155.497 | 1.01[08] | 1.06[08] | $f12sp2$ 011$e$..09 |
| $4f^{12}5s5p^2\ (^3F)\ ^2D^b_{5/2}$ | 154.937 | 156.738 | 3.72[06] | 3.67[06] | $f12sp2$ 010$k$..05 |
| $4f^{12}5s5p^2\ (^3F)\ ^4F^a_{7/2}$ | 153.391 | 152.338 | 4.01[07] | 4.70[07] | $f12sp2$ 010$i$..07 |
| $4f^{12}5s5p^2\ (^3F)\ ^2F^b_{5/2}$ | 151.677 | 150.612 | 1.54[07] | 1.33[07] | $f12sp2$ 000$i$..05 |
| $4f^{12}5s5p^2\ (^1I)\ ^2H^a_{9/2}$ | 145.059 | 143.086 | 2.08[08] | 2.25[08] | $f12sp2$ 011$n$..09 |
| | $4f^{14}5s\ ^2S_{1/2}$-$4f^{14}5p$ $LSJ$ transitions in Pm-like $Au^{18+}$ ion | | | | |
| $4f^{14}5p\ (^1S)\ ^2P_{1/2}$ | 291.148 | 290.587 | 4.08[10] | 3.78[10] | $f145p$ 0101..01 |
| $4f^{14}5p\ (^1S)\ ^2P_{3/2}$ | 185.663 | 186.974 | 3.15[11] | 2.89[11] | $f145p$ 0001..03 |
| | $4f^{14}5s\ ^2S_{1/2}$-$4f^{12}5s^25p$ $LSJ$ transitions in Pm-like $Au^{18+}$ ion | | | | |
| $4f^{12}5s^25p\ (^3P)\ ^4D_{1/2}$ | 163.824 | 166.883 | 9.72[07] | 9.38[07] | $f12s2p$ 0501..01 |
| $4f^{12}5s^25p\ (^1S)\ ^2P_{1/2}$ | 143.132 | 144.090 | 5.89[08] | 4.09[08] | $f12s2p$ 0301..01 |
| $4f^{12}5s^25p\ (^3P)\ ^2P_{1/2}$ | 123.071 | 125.318 | 9.33[06] | 7.28[06] | $f12s2p$ 0104..01 |
| $4f^{12}5s^25p\ (^1S)\ ^2P_{3/2}$ | 109.978 | 110.541 | 1.79[09] | 1.66[09] | $f12s2p$ 0001..03 |

about 227 and 233 Å are formed by $4f^{12}5s^25p$-$4f^{12}5s5p^2$ transitions with $A_r$ values about 110 (in units of $10^9\ s^{-1}$). The line created by the $4f^{14}5s\ ^2S_{1/2}$-$4f^{14}5p\ ^2P_{3/2}$ transition with $\lambda = 260.83$ Å is separated from the bulk of the emission in the region between 230 and 245 Å. The line created by the $4f^{14}5s\ ^2S_{1/2}$-$4f^{14}5p\ ^2P_{1/2}$ transition with $\lambda = 349.56$ Å is in a region of weak lines and is not shown in the figure.

The spectrum of Pm-like $Au^{18+}$ is shown in the bottom panel of Fig. 4, and it looks similar to the beam-foil spectrum of Au at an ion-beam energy of 20 MeV displayed in Fig. 3 of Ref. [5]. The main peak is at 170 Å. The line created by the $4f^{14}5s\ ^2S_{1/2}$-$4f^{14}5p\ ^2P_{3/2}$ transition with $\lambda = 185.66$ Å is separated from the bulk of the emission, while the authors of Ref. [5] put this line inside. There are other small peaks shown in Fig. 3 of Ref. [5] that displays the calculated line due to the $4f^{14}5s\ ^2S_{1/2}$-$4f^{14}5p\ ^2P_{1/2}$ transition. We do not show the $4f^{14}5s\ ^2S_{1/2}$-$4f^{14}5p\ ^2P_{1/2}$ transition at $\lambda = 291.15$ Å, which is located in a region of weak lines. The $4f^{14}5s\ ^2S_{1/2}$-$4f^{14}5p\ ^2P_{1/2}$ transition has an intensity of 20 (in units of $10^9\ s^{-1}$), while the main peak intensity is larger than 220 (in units of $10^9\ s^{-1}$). The intense peaks at about 165 and 179 Å are formed by $4f^{12}5s^25p$-$4f^{12}5s5p^2$ transitions.

A comparison of the spectra in Fig. 4 shows remarkable similarities: Both spectra are dominated by a main peak and contain various intense lines separated from the bulk emission, and both spectra display a second area of emission albeit with small intensity. Both spectra are mainly formed by the $4f^{12}5s^25p$-$4f^{12}5s5p^2$ transitions. A smaller fraction of lines is due to the $4f^{13}5s^2$-$4f^{13}5s5p$ transitions, and two lines are from the $4f^{14}5s$-$4f^{14}5p$ transitions.

## VI. CONCLUSION AND UNCERTAINTY ESTIMATES

We studied previously the properties of $4f$-core-excited states in Refs. [32–36], however, we never investigated the properties of systems with a different number of $4f^n$-core-excited states, such as $4f^{14}5s$, $4f^{14}5p$, $4f^{13}5s^2$, $4f^{13}5s5p$, $4f^{12}5s^25p$, and $4f^{12}5s5p^2$. Even the $4f^{11}5s^25p^2$, $4f^{12}5s5p^3$, $4f^{10}5s^25p^3$, $4f^{10}5s5p^4$ configurations in the case of Pm-like $W^{13+}$ were included in our considerations

To study the properties of Pm-like ions we use the RMBPT code, the COWAN code, and the HULLAC code. We used these codes previously [32–36] to check the accuracy of our calculations. We did not succeed to use the high-accuracy all-order code to evaluate the properties of the $4f^{14}nl$ states as we succeeded in the case the $4f^{14}5p^6nl$ states of Tm-like $W^{5+}$ [32]. Our failure to use the all-order code for the $4f^{14}nl$ states in Pm-like ions is due to the nonstability of the $4f^{14}$ core state. However, we implemented two versions of the second-order RMBPT with Dirac-Fock (DF) and Breit-Dirac-Fock (BDF) potentials to evaluate the energies and wavelengths $4f^{14}nl$ states in Pm-like ions.

The energies of the excited $4f^{14}nl$ states and wavelengths of the $4f^{14}5s\ ^2S_{1/2}$-$4f^{14}5p\ ^2P_J$ transitions were presented in Tables I and II, respectively. The second-order correlation contributions listed in Table I for $4f^{14}nl$ states in Pm-like

$W^{13+}$ are equal to 0.8%–1.1%. The difference in the $4f^{14}nl$ RMBPT energies ($E^{(2)}_{\rm tot}$ and $E^{(2B)}_{\rm tot}$) calculated with the DF and BDF potentials differs by 0.01%.

The results given in column Theory of Table II are the only theoretical results published previously for the Pm-like ions [5]; which were obtained using the MR-MP approach. The comparison of the wavelengths using our two versions of the RMBPT codes and the MR-MP approach presented in Table II shows a 0.2%–2.2% disagreement for the $4f^{14}5s\ ^2S_{1/2}$-$4f^{14}5p\ ^2P_{1/2}$ transition and a 0.2%–0.7% disagreement for the $4f^{14}5s\ ^2S_{1/2}$-$4f^{14}5p\ ^2P_{3/2}$ transition. Results in column COWAN of Table II are evaluated using the COWAN code, which included the $4f^{14}nl$ excited states as well the $4f^{15-k-n}5s^k5p^n$ core-excited states. The results given in columns RMBPT and COWAN of Table II are in excellent agreement (0.04%–0.18%) for the $4f^{14}5s\ ^2S_{1/2}$-$4f^{14}5p\ ^2P_{1/2}$ transition, except the results for the ions with $Z = 74$–$77$ where the difference is 0.5%–1.5%. The largest difference (2.2%) for the $4f^{14}5s\ ^2S_{1/2}$-$4f^{14}5p\ ^2P_{3/2}$ transition is found for the ion with $Z = 92$, while the RMBPT and MR-MP wavelengths are in excellent agreement (0.05%) for Pm-like uranium. Despite the good agreement among the theoretical results, some disagreement with experimental data was observed. In fact, the disagreement between theory and measurement was already noted earlier and it was doubted whether the line identification was correct [5]. This doubt was reiterated in [37]. Our calculations reinforce that there is a significant difference with the experimental values, which creates further doubt that the line identifications in the measurements are correct.

The COWAN and HULLAC codes were used to determine the uncertainties in wavelengths and weighted transition rates for transitions between the $4f$-core-excited states in Pm-like $W^{13+}$ and transition between the $4f^{14}5s\ ^2S_{1/2}$ state and the $4f$-core-excited states in Pm-like $Au^{18+}$. The comparison of the wavelengths given in columns COWAN and HULLAC of Table V shows good agreement (0.2%–1.0%) for most of transitions except for two transitions, which differ by about 1.9%. The difference in the weighted transition rates displayed in columns COWAN and HULLAC of Table V is about 2%–20% for most of transitions except for transitions with smallest $gA_r$ values.

Energies, lifetimes, and sums of radiative decays for the low-lying states in Pm-like $W^{13+}$ ion are tabulated in Tables III and IV. To find out the uncertainties in energies and lifetimes of the results given in these tables, we ran additional calculations using a smaller basis set without including the $4f^{11}5s^25p^2 + 4f^{11}5s5p^3$ and $4f^{10}5s^25p^3 + 4f^{10}5s5p^5$. The contribution of these states for the energies and lifetime of the $4f^{14}5s, 4f^{14}5p, 4f^{13}5s^2, 4f^{13}5p^2, 4f^{12}5s^25p, 4f^{12}5p^3$, and $4f^{12}5s5p^2$ states is not large. The difference in energies was about 0.1%–1%, while the difference in lifetimes was about 1%–5%.

These atomic data are particulary important for fusion research where tungsten is produced in low ionization stages.

## ACKNOWLEDGMENTS

This research was sponsored by DOE under the OFES Grant No. DE-FG02-08ER54951 and in part under the NNSA Cooperative Agreement No. DE-NA0001984. Work at the Lawrence Livermore National Laboratory was performed under auspices of the DOE under Contract No. DE-AC52-07NA-27344.

[1] N. Huntemann, M. Okhapkin, B. Lipphardt, S. Weyers, Chr. Tamm, and E. Peik, Phys. Rev. Lett. **108**, 090801 (2012).
[2] J. C. Berengut, V. A. Dzuba, V. V. Flambaum, and A. Ong, Phys. Rev. Lett. **106**, 210802 (2011).
[3] L. J. Curtis and D. G. Ellis, Phys. Rev. Lett. **45**, 2099 (1980).
[4] C. E. Theodosiou and V. Raftopoulos, Phys. Rev. A **28**, 1186 (1983).
[5] M. J. Vilkas, Y. Ishikawa, and E. Träbert, Phys. Rev. A **77**, 042510 (2008).
[6] A. E. Kramida and T. Shirai, At. Data Nucl. Data Tables **95**, 305 (2009).
[7] A. Kramida, Can. J. Phys. **89**, 551 (2011).
[8] R. Hutton, Y. Zou, J. R. Almandos, C. Biedermann, R. Radtke, A. Greier, and R. Neu, Nucl. Instrum. Methods Phys. Res. B **205**, 114 (2003).
[9] S. Wu and R. Hutton, Can. J. Phys. **86**, 125 (2008).
[10] W. R. Johnson, S. A. Blundell, and J. Sapirstein, Phys. Rev. A **37**, 307 (1988).
[11] J. Clementson, P. Beiersdorfer, G. Brown, M. Gu, H. Lundberg, Y. Podpaly, and E. Träbert, Can. J. Phys. **89**, 571 (2011).
[12] P. Beiersdorfer, J. K. Lepson, M. B. Schneider, and M. P. Bode, Phys. Rev. A **86**, 012509 (2012).
[13] C. Suzuki, C. S. Harte, D. Kilbane, T. Kato, H. A. Sakaue, I. Murakami, D. Kato, K. Sato, N. Tamura, S. Sudo *et al.*, J. Phys. B **44**, 175004 (2011).
[14] C. Suzuki, C. S. Harte, D. Kilbane, T. Kato, H. A. Sakaue, I. Murakami, D. Kato, K. Sato, N. Tamura, S. Sudo *et al.*, AIP Conf. Proc. **1438**, 197 (2012).
[15] J. Clementson, P. Beiersdorfer, E. W. Magee, H. S. McLean, and R. D. Wood, J. Phys. B **43**, 144009 (2010).
[16] J. Clementson, P. Beiersdorfer, and M. F. Gu, Phys. Rev. A **81**, 012505 (2010).
[17] J. Clementson, P. Beiersdorfer, G. V. Brown, and M. F. Gu, Phys. Scr. **81**, 015301 (2010).
[18] P. Beiersdorfer, G. V. Brown, J. Clementson, J. Dunn, K. Morris, E. Wang, R. L. Kelley, C. A. Kilbourne, F. S. Porter, M. Bitter *et al.*, Rev. Sci. Instrum. **81**, 10E323 (2010).
[19] C. S. Harte, C. Suzuki, T. Kato, H. A. Sakaue, D. Kato, K. Sato, N. Tamura, S. Sudo, R. D'Arcy, and E. Sokell, J. Phys. B **43**, 205004 (2010).
[20] J. Clementson and P. Beiersdorfer, Phys. Rev. A **81**, 052509 (2010).
[21] P. Beiersdorfer, J. Clementson, J. Dunn, M. F. Gu, K. Morris, Y. Podpaly, E. Wang, M. Bitter, R. Feder, K. Hill *et al.*, J. Phys. B **43**, 144008 (2010).

[22] J. Clementson, P. Beiersdorfer, A. L. Roquemore, C. H. Skinner, D. K. Manseld, K. Hartzfeld, and J. K. Lepson, Rev. Sci. Instrum. **81**, 10E326 (2010).
[23] M. Reinke, P. Beiersdorfer, N. T. Howard, E. W. Magee, Y. Podpaly, J. E. Rice, and J. L. Terry, Rev. Sci. Instrum. **81**, 10D736 (2010).
[24] J. Yanagibayashi, T. Nakano, A. Iwamae, H. Kubo, M. Hasuo, and K. Itami, J. Phys. B **43**, 144013 (2010).
[25] Y. Podpaly, J. Clementson, P. Beiersdorfer, J. Williamson, G. V. Brown, and M. F. Gu, Phys. Rev. A **80**, 052504 (2009).
[26] U. I. Safronova and W. R. Johnson, Phys. Rev. A **69**, 052511 (2004).
[27] U. I. Safronova, W. R. Johnson, and M. S. Safronova, Phys. Rev. A **76**, 042504 (2007).
[28] S. A. Blundell, W. R. Johnson, M. S. Safronova, and U. I. Safronova, Phys. Rev. A **77**, 032507 (2008).
[29] R. D. Cowan, *The Theory of Atomic Structure and Spectra* (University of California Press, Berkeley, 1981).
[30] B. C. Fawcett, N. J. Peacock, and R. D. Cowan, J. Phys. B **1**, 295 (1968).
[31] http://das101.isan.troitsk.ru/cowan.htm.
[32] U. I. Safronova and A. S. Safronova, Phys. Rev. A **85**, 032507 (2012).
[33] U. I. Safronova, A. S. Safronova, and P. Beiersdorfer, J. Phys. B **45**, 085001 (2012).
[34] U. I. Safronova and A. S. Safronova, Phys. Rev. A **84**, 012511 (2011).
[35] U. I. Safronova and M. S. Safronova, Phys. Rev. A **79**, 032511 (2009).
[36] V. A. Dzuba, U. I. Safronova, and W. R. Johnson, Phys. Rev. A **68**, 032503 (2003).
[37] E. Träbert, M. J. Vilkas, and Y. Ishikawa, J. Phys.: Conf. Ser. **163**, 012017 (2009).